

Critical mingling and universal correlations in binary active liquids

Nicolas Bain¹ and Denis Bartolo¹

¹*Univ Lyon, Ens de Lyon, Univ Claude Bernard,
CNRS, Laboratoire de Physique, F-69342 Lyon, France*

(Dated: February 13, 2017)

Ensembles of driven or motile bodies moving along opposite directions are generically reported to self-organize into strongly anisotropic lanes. We quantitatively elucidate this behavior for binary mixtures of self-propelled bodies targeting opposite directions. We evidence a critical phase transition between a mingled state and a phase-separated lane state specific to active particles. We then theoretically explain universal long-range structural correlations found in both the mingled state and binary mixtures of oppositely driven colloids.

Should you want to mix two groups of pedestrians, or two ensembles of colloidal beads, one of the worst possible strategies would be pushing them towards each other. Both experiments and numerical simulations have demonstrated the segregation of oppositely driven Brownian particles into parallel lanes [1–5]. Even the tiniest drive results in the formation of finite slender lanes which exponentially grow with the driving strength [5]. The same qualitative phenomenology is consistently observed in pedestrian counterflows [6–10]. From our daily observation of urban traffic to laboratory experiments, the emergence of counter propagating lanes is one of the most robust phenomena in population dynamics, and has been at the very origin of the early description of pedestrians as granular materials [11, 12]. However, a description as isotropic grains is usually not sufficient to account for the dynamics of interacting motile bodies [13–15]. From motility-induced phase separation [15], to giant density fluctuations in flocks [13, 16, 17], to pedestrian scattering [18, 19], the most significant collective phenomena in active matter stem from the interplay between their position *and* orientation degrees of freedom.

In this communication, we address the phase behavior of a binary mixture of active particles targeting opposite directions. Building on a prototypical model of self-propelled bodies with repulsive interactions, we numerically evidence two nonequilibrium steady states: (i) a lane state where the two populations maximize their flux and phase separate, and (ii) a mixed state where all motile particles mingle homogeneously. We show that these two distinct states are separated by a genuine critical phase transition, thereby stressing on the qualitative difference between driven and active binary liquids. However, we also demonstrate algebraic density correlations in the homogeneous phase, akin to that recently reported for oppositely driven Brownian particles [20]. We analytically account for these long-range structural correlations and elucidate their universality.

RESULTS

We consider an ensemble of N self-propelled particles characterized by their instantaneous positions $\mathbf{r}_i(t)$ and

orientations $\hat{\mathbf{p}}_i(t) = (\cos \theta_i, \sin \theta_i)$, where $i = 1, \dots, N$ (in all that follows $\hat{\mathbf{x}}$ stands for $\mathbf{x}/|\mathbf{x}|$). Each particle moves along its orientation vector at constant speed ($|\dot{\mathbf{r}}_i| = 1$), and their equations of motion take the simple form:

$$\dot{\mathbf{r}}_i = \hat{\mathbf{p}}_i, \quad (1)$$

$$\dot{\theta}_i = -\partial_{\theta_i} \mathcal{V}(\theta_i) + \sum_j T_{ij}. \quad (2)$$

We separate the particle ensemble into two groups of equal size following either the direction $\Theta_i = 0$ (right movers) or π (left movers) according to a harmonic angular potential $\mathcal{V}(\theta_i) = \frac{H}{2}(\theta_i - \Theta_i)^2$. The motile particles interact at a distance through a repelling torque: $T_{ij} = -\partial_{\theta_i} \mathcal{E}_{ij}$, where the effective angular energy simply reads $\mathcal{E}_{ij} = -B(r_{ij})\hat{\mathbf{p}}_i \cdot \hat{\mathbf{r}}_{ij}$. As sketched in Fig. 1a, this interaction promotes the orientation of $\hat{\mathbf{p}}_i$ along the direction of the center-to-center vector $\mathbf{r}_{ij} = (\mathbf{r}_i - \mathbf{r}_j)$: as they interact particles turn their back to each other. The spatial decay of the interactions is given by: $B(r_{ij}) = B(1 - r_{ij}/(a_i + a_j))$, where B is a finite constant if $r_{ij} < (a_i + a_j)$ and 0 otherwise. The interaction ranges a_i are chosen to be polydisperse in order to avoid the specifics of crystallization, and we make the classic choice $a = 1$ or 1.4 for one in every two particles. We note that this type of interaction is not only common to heuristic models of interacting pedestrians [19], or animals [21] but also relevant to synthetic active particles such as some self-propelled colloids [22]. Unlike models of *driven* colloids or grains interacting via repulsive potentials [1, 5, 20], Eqs. (1) and (2) are not invariant upon Galilean boosts, and therefore are not suited to describe particles moving at different speeds along the same preferred direction.

We numerically solve Eqs. (1) and (2) using forward Euler integration with a time step of 10^{-2} , and a prune-and-sweep algorithm for neighbour summation. We use a rectangular simulation box of aspect ratio $L_x = 2L_y$ with periodic boundary conditions in both directions. We also restrain our analysis to $H = 1$, leaving two control parameters that are the repulsion strength B and the overall density $\bar{\rho}$. The following results correspond to simulations with N comprised between 493 and 19730 particles.

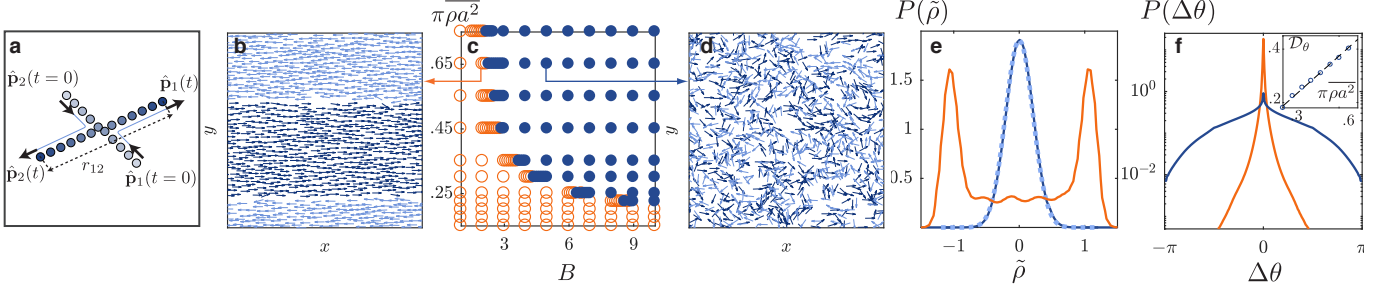


FIG. 1. Phase behavior. (a) Trajectories of two particles interacting solely via a repulsive torque as defined in Eq. (2) with $B = 5$. The post-collision orientations $\hat{\mathbf{p}}_i(t)$ are along the center to center axis \mathbf{r}_{ij} . (b) and (d) Snapshots of a square window at the center of the simulation box ($L_x = 168$, $N = 1973$, $\pi\bar{\rho}a^2 = 0.65$), respectively in the lane ($B = 2$) and the homogeneous ($B = 5$) states. The arrows indicate the instantaneous position and orientation of the particles. Dark blue : right movers. Light blue : left movers. (b) Phase diagram. $\pi\bar{\rho}a^2$ is the particle area fraction. Filled symbols: homogeneous state. Open symbols: lanes. (e) Probability -distribution of the density difference $\tilde{\rho} = \rho_r - \rho_l$. Light orange line: $B = 2$, $\pi\bar{\rho}a^2 = 0.65$. Dark blue line: $B = 5$, $\pi\bar{\rho}a^2 = 0.65$. Dashed line: best Gaussian fit. (f) P.d.f. of the orientational fluctuations around the preferred orientation (lin-log plot). Same parameters and colors as in (e). Inset : orientational diffusivity \mathcal{D}_θ in the homogeneous state at a fixed repulsion magnitude ($B = 5$) and different particle area fraction $\pi\bar{\rho}a^2$. Dashed line : best linear fit.

Critical mingling.

Starting from random initial conditions, we observe two clearly distinct stationary states illustrated in Figs. 1b and 1d. At low density and/or weak repulsion the system quickly phase separates. Computing the local density difference between the right and left movers $\tilde{\rho}(\mathbf{r}, t) = \rho_r(\mathbf{r}, t) - \rho_l(\mathbf{r}, t)$, we show that this dynamical state is characterized by a strongly bimodal density distribution, see Fig. 1e. The left and right movers quickly self-organize into counter-propagating lanes separated by a sharp interface, Fig. 1b. In each stream, virtually no particle interact and most of the interactions occur at the interface. As a result the particle orientations are very narrowly distributed around their mean value, Fig. 1f. In stark contrast, at high density and/or strong repulsion, the motile particles do not phase separate. Instead, the two population mingle and continuously interact to form a homogeneous liquid phase with Gaussian density fluctuations, and much broader orientational fluctuations, Figs. 1d, 1e, and 1f. This behavior is summarized by the phase diagram in Fig. 1c. Although phase separation is most often synonymous of first order transition in equilibrium liquids, we now argue that the lane and the mingle states are two genuine non-equilibrium phases separated by a critical line in the $(B, \bar{\rho})$ plane. To do so, we first introduce the following order parameter:

$$\langle W \rangle = \langle 1 - \cos(\theta_i - \Theta_i) \rangle_i. \quad (3)$$

$\langle W \rangle$ vanishes in the laning phase where on average all particles follow their preferred direction, and takes a non zero value otherwise. We show in Fig. 2a how $\langle W \rangle$ increases with the repulsion strength B at constant $\bar{\rho}$. For $\pi\bar{\rho}a^2 = 0.65$ the order parameter averages to zero below $B_c = 2.17 \pm 0.02$, while above B_c it sharply increases as $W \sim |B - B_c|^\beta$, with $\beta = 0.33 \pm 0.07$, Fig. 2b. This scal-

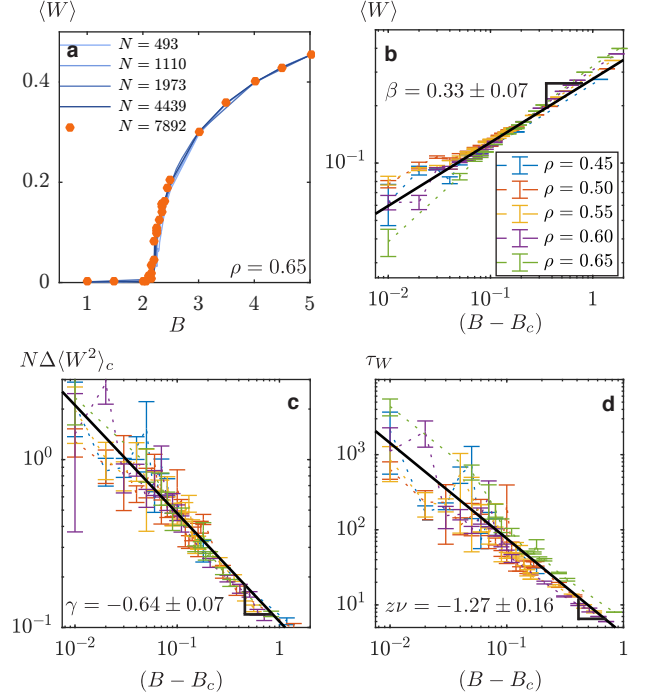


FIG. 2. Critical transition from laned to homogeneous liquid states. (a) and (b) Linear and log plots of the order parameter $\langle W \rangle$ defined in Eq. (3). (a): $\pi\bar{\rho}a^2 = 0.65$, the bifurcation curves collapse for five system sizes. (b), (c) and (d) Log plots at five densities for a box of length $L_x = 336$ (N ranges from 5462 to 7892). (c) Fluctuations of the order parameter plotted versus $B - B_c$ for the same densities as in (b). The fluctuations are defined as $\Delta\langle W^2 \rangle_c \equiv \langle W^2 \rangle_c(B) - \langle W^2 \rangle_c(B \rightarrow \infty)$. (d) Correlation time τ_W plotted against $B - B_c$. The correlation time is defined as $\langle W(t + \tau_W)W(t) \rangle_c = \frac{1}{2} \langle W^2(t) \rangle_c$. All error bars correspond to two standard deviations. The error on the estimate of the exponents correspond to one standard deviation after considering linear fits for each density.

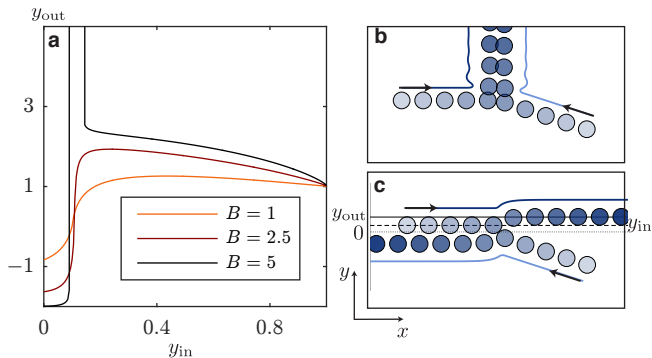


FIG. 3. Collision between left and right movers. (a) The transverse displacement y_{out} is plotted as a function of the impact parameter y_{in} (defined in (c)), for different values of the repulsion strength B . Initial conditions : a right mover with an orientation $\theta_r = 0$ and a left mover with $\theta_l = \pi - \pi/10$ are vertically placed at $+y_{\text{in}}$ and $-y_{\text{in}}$. Their x coordinate is chosen so that they start interacting at $t = 0$. (b) and (c) Trajectories of two colliding particles in the presence of an alignment field. The trajectories before contact are prolongations of the incoming orientations, both interactions and alignment field are only turned on at contact. (b) A pair of particles targeting opposite directions travelling in the transverse direction $\hat{\mathbf{y}}$ ($B = 5$, $y_{\text{in}} = 0.125$). (c) Typical scattering trajectory ($B = 5$, $y_{\text{in}} = 0.75$). y_{in} (resp. y_{out}) is the initial (resp. final) vertical position of the right mover. Note the strong transverse deviation.

ing law suggests a genuine critical behavior. We further confirm this hypothesis in Fig. 2c, showing that the fluctuations of the order parameter diverge as $|B - B_c|^\gamma$, with $\gamma = -0.64 \pm 0.07$. Deep in the homogeneous phase the fluctuations plateau to a constant value of the order of $1/N$. Finally, the criticality hypothesis is unambiguously ascertained by Fig. 2d, which shows the power-law divergence of the correlation time of $\langle W \rangle(t)$: $\tau_W \sim |B - B_c|^{z\nu}$ with $z\nu = -1.21 \pm 0.16$.

The existence of two distinct phases seemingly contradicts the recent prediction by Glanz and Löwen. In [5] they showed that ensembles of oppositely driven particles merely crossover from a homogeneous to a lane state upon increasing the driving amplitude. These results are however not contradictory. Instead, this marked difference demonstrates the crucial role of self-propulsion at constant speed. In the overdamped limit, the collision between two oppositely driven colloids would at most shift their position over an interaction diameter [23]. Conversely, collisions between self-propelled particles result in persistent deviations transverse to their preferred trajectories for a finite set of impact parameters, see Fig. 3a and Supplemental Materials [24]. This persistent scattering stems from the competition between repulsion and alignment. When these two contributions compare, bound pairs of oppositely moving particles can even form and steadily propel along the transverse direction $\hat{\mathbf{y}}$, Figs. 3a and 3b. We stress that this behavior is not peculiar to this two-body setting. Persistent trans-

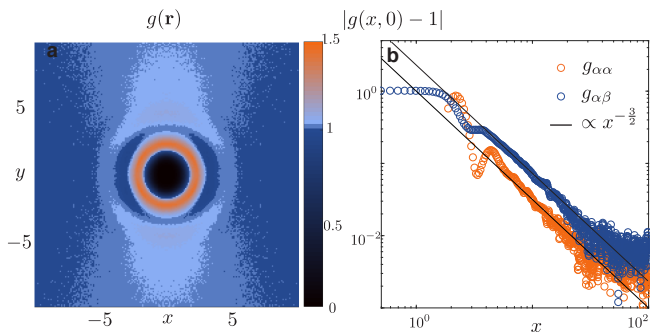


FIG. 4. Structural correlations. (a) Overall pair correlation function deep in the homogeneous phase ($B = 5$). (b) Plot of the longitudinal decay of the density auto- (dark blue) and cross- (light orange) correlation functions at $y = 0$. Black line : algebraic decay $x^{-3/2}$.

verse motion of bound pair is clearly observed at the onset of laning. We therefore strongly suspect the resulting enhanced mixing to cause the sharp melting of the lane state.

Long-range correlations in mingled liquids.

We now evidence long-range structural correlations in this novel active-liquid phase, and analytically demonstrate their universality. The overall pair correlation function of the active liquid, $g(\mathbf{r})$, is plotted in Fig. 4a. At a first glance, deep in the homogeneous phase, the few visible oscillations would suggest a simple anisotropic liquid structure. However, denoting α and β the preferred direction of the populations (left or right), we find that the asymptotic behaviors of all pair correlation functions $g_{\alpha\beta}(x, y = 0)$ decay algebraically as $|1 - g_{\alpha\beta}(x, 0)| \sim x^{-\nu_x}$ with $\nu_x \sim 1.5$, Fig. 4b. This power-law behavior is very close to that reported in numerical simulations [4] and fluctuating density functional theories of oppositely driven colloids at finite temperature [20].

Hydrodynamic description

In order to explain the robustness of these long-range correlations, we first provide a hydrodynamic description of the mingle state, and compute its structural response to random fluctuations. We first observe that the orientational diffusivity of the particles increases linearly with the average density $\bar{\rho}$ in Fig. 1f inset. This behaviour indicates that binary collisions set the fluctuations of this active liquid, and hence suggests using a Boltzmann kinetic-theory framework, see e.g [25, 26] for an active-matter perspective. In the large B limit, the microscopic interactions are accounted for by a simplified scattering rule anticipated from Eq. (2) and confirmed by the inspection of typical trajectories (see Fig. 1a). Upon

binary collisions the self-propelled particles align their orientation with the center-to-center axis regardless of their initial orientation and external drive. Assuming molecular chaos and binary collisions only, the time evolution of the one-point distribution functions $\psi_\alpha(\mathbf{r}, \theta, t)$ reads:

$$\partial_t \psi_\alpha + \nabla \cdot [\hat{\mathbf{p}} \psi_\alpha] + \partial_\theta \left[\partial_\theta (\hat{\mathbf{p}} \cdot \hat{\mathbf{h}}_\alpha) \psi_\alpha \right] = \mathcal{I}_\alpha^{\text{coll}}. \quad (4)$$

The convective term on the l.h.s stems from self-propulsion, the third term accounts for alignment with the preferred direction $\hat{\mathbf{h}}_\alpha = \hat{\mathbf{x}}$ (resp. $-\hat{\mathbf{x}}$) for the right (resp. left) movers. Using the simplified scattering rule to express the so-called collision integral on the r.h.s, we can establish the dynamical equations for the density fluctuations $\delta\rho_\alpha$ around the average homogeneous state (see Methods for technical details). Within a linear response approximation, they take the compact form:

$$\partial_t \delta\rho_\alpha(\mathbf{r}, t) + \nabla \cdot (\mathbf{J}_\alpha + \tilde{\mathbf{J}}) = 0, \quad (5)$$

where \mathbf{J}_α describes the convection and the collision-induced diffusion of the α species, and $\tilde{\mathbf{J}}$ is the coupling term, crucial to the anomalous fluctuations of the active liquid:

$$\mathbf{J}_\alpha = v_0 \hat{\mathbf{h}}_\alpha \delta\rho_\alpha - \mathbf{D} \cdot \nabla \delta\rho_\alpha, \quad (6)$$

$$\tilde{\mathbf{J}} = -\tilde{v} \hat{\mathbf{h}}_\alpha \delta\bar{\rho} - \tilde{\mathbf{D}} \cdot \nabla \delta\bar{\rho}, \quad (7)$$

The two anisotropic diffusion tensors \mathbf{D} and $\tilde{\mathbf{D}}$ are diagonal and their expression is provided in [24] together with all the hydrodynamic coefficients. $\tilde{\mathbf{J}}$ is a particle current stemming from the fluctuations of the other species and has two origins. The first term arises from the competition between alignment along the driving direction $\hat{\mathbf{h}}_\alpha$ and orientational diffusion caused by the collisions: the higher the local density $\bar{\rho}$, the smaller the longitudinal current. The second term originates from the pressure term $\propto \nabla \bar{\rho}$: a local density gradient results in a net flow of both species (see Methods for details). This diffusive coupling is therefore generic and enters the description of any binary compressible fluid.

By construction this hydrodynamic description alone cannot account for any structural correlation. In order to go beyond this mean-field picture we classically account for fluctuations by adding a conserved noise source to Eqs. (5) and compute the resulting density-fluctuation spectrum [13]. At the linear response level, without loss of generality [24], we can restrain ourselves to the case of an isotropic additive white noise of variance $2T$. Going to Fourier space, and after lengthy yet straightforward algebra we obtain in the long wavelength limit [24]:

$$\langle |\delta\rho_\alpha(\mathbf{q})|^2 \rangle \propto \frac{q_y^4 (D_y + \tilde{D}_y)^2 + q_x^2 (v_0 - \tilde{v})^2}{q_y^4 D_y (D_y + 2\tilde{D}_y) + q_x^2 v_0 (v_0 - 2\tilde{v})} \quad (8)$$

with $\delta\rho(\mathbf{q}) = \int \delta\rho(\mathbf{r}) \exp(-i\mathbf{q} \cdot \mathbf{r}) d\mathbf{r}$, and where $\langle \cdot \rangle$ is a noise average. The cross-correlation $\langle \delta\rho_\alpha(\mathbf{q}) \delta\rho_\beta(-\mathbf{q}) \rangle$

has a similar form, see Supplementary Note. Even though the above hydrodynamic description of active particles qualitatively differs from that of driven colloids, they both yield the same fluctuation spectra [20, 24]. The non analyticity of Eq. (8) in the long wavelength limit translates in an algebraic decay of the density correlations in real space: $\langle |\rho_\alpha(0, 0) \rho_\alpha(x, 0)| \rangle = |1 - g_{\alpha\alpha}(x)| \sim x^{-\frac{3}{2}}$, in agreement with our numerical simulations, Fig. 4b. We emphasize that this prediction is not specific to the small-density regime and is expected to be very robust to the microscopic details of the interactions. While the above theory is valid in the limit of strong repulsion and small densities, in a supplementary document we use a kinetic theory valid in the opposite limit [13], where the particle density is very large while the repulsion remains finite [24]. We recover the same hydrodynamic theory which as it turns out could have been also phenomenologically anticipated using conservation law and symmetry considerations [16].

DISCUSSION

A number of different non-equilibrium phenomena could result in a non analytic form of the structure factor as $q \rightarrow 0$, and hence to algebraic density correlations [27]. However, inspecting Eq. (8), we can identify the very ingredients required to yield the universal $x^{-\frac{3}{2}}$ power law found both in active and driven binary mixtures. Starting from two opposite populations undergoing longitudinal convection and diffusion (\mathbf{J}_α in Eq. (5)), the minimal coupling between the density excitations must either have the form of a longitudinal convective current $\propto \partial_x \bar{\rho}$, or of a transverse diffusive flux $\propto \partial_y^2 \bar{\rho}$. Both ingredients are present in our model ($\tilde{\mathbf{J}}$ in Eqs. (5)). While the convective coupling is specific to motile units, collision-induced transverse diffusion holds in any liquid made of particles interacting via short range interactions (away from dynamical arrest).

In conclusion, we have demonstrated how the interplay between orientational and translational degrees of freedom, inherent to motile bodies, results in a critical transition between a phase separated and a mingled state in binary active mixtures. In addition we have singled out the very mechanisms responsible for long-range structural correlations in any ensemble of particles driven towards opposite directions, should they be passive colloids or self-propelled agents.

METHODS

Let us summarize the main steps of the kinetic theory employed to establish Eqs. (5) (6), (7). The so-called collision integral on the r.h.s of Eq. (4) includes two contributions which translate the behavior illustrated in

Fig. 1a:

$$\mathcal{I}_\alpha^{\text{coll}} = \mathcal{D}_{\text{in}} \rho_\alpha(\mathbf{r}) \bar{\rho}(\mathbf{r} - 2a\hat{\mathbf{p}}) - \mathcal{D}_{\text{out}} \bar{\rho}(\mathbf{r}) \psi_\alpha(\mathbf{r}, \theta). \quad (9)$$

The first term indicates that a collision with any particle located at $(\mathbf{r} - 2a\hat{\mathbf{p}})$ reorients the α particles along $\hat{\mathbf{p}}(\theta)$ at a rate \mathcal{D}_{in} . The second term accounts for the random reorientation, at a rate \mathcal{D}_{out} , of a particle aligned with $\hat{\mathbf{p}}(\theta)$ upon collision with any other particle. Within a two-fluid picture, the velocity and nematic texture of the α particles are given by $\mathbf{v}_\alpha = \rho_\alpha^{-1} \langle \hat{\mathbf{p}} \rangle_\theta$ and $\mathbf{Q}_\alpha = \rho_\alpha^{-1} \langle \hat{\mathbf{p}}\hat{\mathbf{p}} - \frac{1}{2}\mathbb{I} \rangle_\theta$. The mass conservation relation, $\partial_t \rho_\alpha + \nabla \cdot (\rho_\alpha \mathbf{v}_\alpha) = 0$, is obtained by integrating Eq. (4) with respect to θ and constrains $(2\pi\mathcal{D}_{\text{in}}) = \mathcal{D}_{\text{out}} \equiv \mathcal{D}$. The time evolution of the velocity field is also readily obtained from Eq. (4):

$$\partial_t(\rho_\alpha \mathbf{v}_\alpha) + \nabla \cdot \left[\rho_\alpha \left(\frac{\mathbb{I}}{2} + \mathbf{Q}_\alpha \right) \right] = \mathcal{F}_\alpha, \quad (10)$$

where the second term on the l.h.s is a convective term stemming from self-propulsion. The force field \mathcal{F}_α on the r.h.s of Eq. (10) reads: $\mathcal{F}_\alpha = \rho_\alpha \left(\frac{\mathbb{I}}{2} - \mathbf{Q}_\alpha \right) \cdot \hat{\mathbf{h}}_\alpha - (a\mathcal{D}\rho_\alpha)\nabla\bar{\rho} - (\mathcal{D}\bar{\rho})\rho_\alpha\mathbf{v}_\alpha$. The first term originates from the alignment of particles along the $\hat{\mathbf{h}}_\alpha$ direction, the second term is a repulsion-induced pressure, and the third one echoes the collision-induced rotational diffusivity of the particles. An additional closure relation between \mathbf{Q}_α , \mathbf{v}_α and ρ_α is required to yield a self-consistent hydrodynamic description. Deep in the homogeneous phase, we make a wrapped Gaussian approximation for the orientational fluctuations in each population [22, 28]. This hypothesis is equivalent to setting $\mathbf{Q}_\alpha = |\mathbf{v}_\alpha|^4 (\hat{\mathbf{v}}_\alpha \hat{\mathbf{v}}_\alpha - \frac{1}{2}\mathbb{I})$ [22, 29]. As momentum is not conserved, the velocity field is not a hydrodynamic variable; in the long wavelength limit the velocity modes relax much faster than the (conserved) density modes. We therefore ignore the temporal variations in Eq. (10) and use this simplified equation to eliminate \mathbf{v}_α in the mass-conservation relation, leading to the mass conservation equation Eq. (5).

REFERENCES

- [1] J. Dzubiella, G. P. Hoffmann, and H. Löwen, Phys. Rev. E **65**, 021402 (2002).
- [2] M. E. Leunissen, C. G. Christova, A.-P. Hynninen, C. P. Royall, A. I. Campbell, A. Imhof, M. Dijkstra, R. van Roij, and A. van Blaaderen, Nature **437**, 235 (2005).
- [3] T. Vissers, A. Wysocki, M. Rex, H. Lowen, C. P. Royall, A. Imhof, and A. van Blaaderen, Soft Matter **7**, 2352 (2011).
- [4] M. Kohl, A. V. Ivlev, P. Brandt, G. E. Morfill, and H. Löwen, Journal of Physics: Condensed Matter **24**, 464115 (2012).
- [5] T. Glanz and H. Löwen, Journal of Physics: Condensed Matter **24**, 464114 (2012).
- [6] S. Older, *Movement of pedestrians on footways in shopping streets* (Traffic engineering & control, 1968).
- [7] S. Milgram, H. Toch, and J. Drury, *Collective behavior: Crowds and social movements* (1969).

- [8] S. Hoogendoorn and W. Daamen, “Self-Organization in Pedestrian Flow,” in *Traffic and Granular Flow '03*, edited by S. P. Hoogendoorn, S. Luding, P. H. L. Bovy, M. Schreckenberg, and D. E. Wolf (Springer Berlin Heidelberg, Berlin, Heidelberg, 2005) pp. 373–382.
- [9] T. Kretz, A. Grünebohm, M. Kaufman, F. Mazur, and M. Schreckenberg, Journal of Statistical Mechanics: Theory and Experiment **2006**, P10001 (2006).
- [10] M. Moussaïd, E. G. Guilloit, M. Moreau, J. Fehrenbach, O. Chabiron, S. Lemerrier, J. Pettré, C. Appert-Rolland, P. Degond, and G. Theraulaz, PLOS Computational Biology **8**, 1 (2012).
- [11] D. Helbing and P. Molnár, Phys. Rev. E **51**, 4282 (1995).
- [12] D. Helbing, I. J. Farkas, and T. Vicsek, Phys. Rev. Lett. **84**, 1240 (2000).
- [13] M. C. Marchetti, J. F. Joanny, S. Ramaswamy, T. B. Liverpool, J. Prost, M. Rao, and R. A. Simha, Rev. Mod. Phys. **85**, 1143 (2013).
- [14] A. Zöttl and H. Stark, Journal of Physics: Condensed Matter **28**, 253001 (2016).
- [15] M. E. Cates and J. Tailleur, Annual Review of Condensed Matter Physics **6**, 219 (2015).
- [16] J. Toner and Y. Tu, Phys. Rev. Lett. **75**, 4326 (1995).
- [17] J. Toner, Y. Tu, and S. Ramaswamy, Annals of Physics **318**, 170 (2005).
- [18] M. Moussaïd, N. Perozo, S. Garnier, D. Helbing, and G. Theraulaz, PLOS ONE **5**, 1 (2010).
- [19] M. Moussaïd, D. Helbing, and G. Theraulaz, Proceedings of the National Academy of Sciences **108**, 6884 (2011).
- [20] A. Poncet, O. Bénichou, V. Démery, and G. Oshanin, ArXiv e-prints (2016), arXiv:1608.00094 [cond-mat.stat-mech].
- [21] I. D. Couzin, J. Krause, N. R. Franks, and S. A. Levin, Nature **433**, 513 (2005).
- [22] A. Bricard, J.-B. Caussin, N. Desreumaux, O. Dauchot, and D. Bartolo, Nature **503**, 95 (2013).
- [23] K. Klymko, P. L. Geissler, and S. Whitelam, Phys. Rev. E **94**, 022608 (2016).
- [24] See Supplemental Materials for further explanations on the persistent transverse scattering, more details on the linearized hydrodynamics in the dilute and large density limits, and derivation of the long-range density correlations.
- [25] A. Peshkov, E. Bertin, F. Ginelli, and H. Chaté, The European Physical Journal Special Topics **223**, 1315 (2014).
- [26] F. Thüroff, C. A. Weber, and E. Frey, Phys. Rev. X **4**, 041030 (2014).
- [27] G. Grinstein, D.-H. Lee, and S. Sachdev, Phys. Rev. Lett. **64**, 1927 (1990).
- [28] H. Seyed-Allaei, L. Schimansky-Geier, and M. R. Ejtehadi, Phys. Rev. E **94**, 062603 (2016).
- [29] A. Bricard, J.-B. Caussin, D. Das, C. Savoie, V. Chikkadi, K. Shitara, O. Chepizhko, F. Peruani, D. Saintillan, and D. Bartolo, Nature Communications **6**, 7470 (2015).

ACKNOWLEDGMENTS

We acknowledge support from ANR grant MiTra and Institut Universitaire de France (D. B.). We thank V. Demery for insightful discussions.

AUTHOR CONTRIBUTIONS

D. B. Designed the research. B.N. performed the numerical simulations. D. B. and N. B. performed the theory, discussed the results and wrote the paper.